IL NUOVO CIMENTO Vol. 24 C, N. 2 Marzo-Aprile 2001

Atmospheric convergence diabatically generated in the CBL over a mountainous peninsula (*)

S. Federico(1), G. A. Dalu(3), L. Casella(1)
C. Bellecci(2) and M. Colacino(3)

(1) *CRATI Scrl, Università della Calabria - 87036 Rende (CS), Italy*
(2) *INFM - Università di Roma "Tor Vergata" Dept. STFE - via di Tor Vergata I-00136 Rome, Italy*
(3) *IFA-CNR - via del Fosso del Cavaliere 100, I-00133 Rome, Italy*

(ricevuto il 20 Ottobre 1999; revisionato il 5 Dicembre 2000; approvato il 20 Dicembre 2000)

Summary. — The mesoscale atmospheric flow is investigated that is diabatically forced by the diurnal warming in the convective boundary layer (CBL) over Calabria, a mountainous peninsula in southern Italy. This study, carried out using a 3D nonlinear numerical model, is concerned with summer time when the large-scale flow is weak. Owing to several favourable conditions, strong sea-breeze and mountain valley flows are developed over this area. The thermal gradients associated with contrast of either mountain peaks-free atmosphere or land-sea merge together generating wide and intense circulation. The results show strong convergence in the lower and divergence in the mid and upper troposphere. The depth of the CBL is of the order of two thousand metres, while the depth of the mesoscale atmospheric response is of the order of the troposphere height, and has a horizontal scale of the order of two Rossby radii. The main effect of such circulation is the reorganisation of the humid air over the region. Indeed the humid air, that comes from the lower levels, is advected upward by breeze circulation, determining the onset of cumulus cloud and triggering summer thunderstorm over the region. The model provides successful simulations of the convective development observed by ground stations.

PACS 92.60.Gn – Winds and their effects.
PACS 92.60.Ry – Climatology.

1. – Introduction

The sea breeze is a common phenomenon in coastal areas, typical of fair weather conditions. It is a diurnal wind with a horizontal extension of the order of 100 km and a vertical response of the order of 1 km. The observed sea breeze intensity, that can reach $10\,\mathrm{ms}^{-1}$, varies depending on several factors such as large-scale wind flows, atmospheric static stability, cloud coverage, land use etc. Opposed to and weaker than sea breeze,

(*) The authors of this paper have agreed to not receive the proofs for correction.

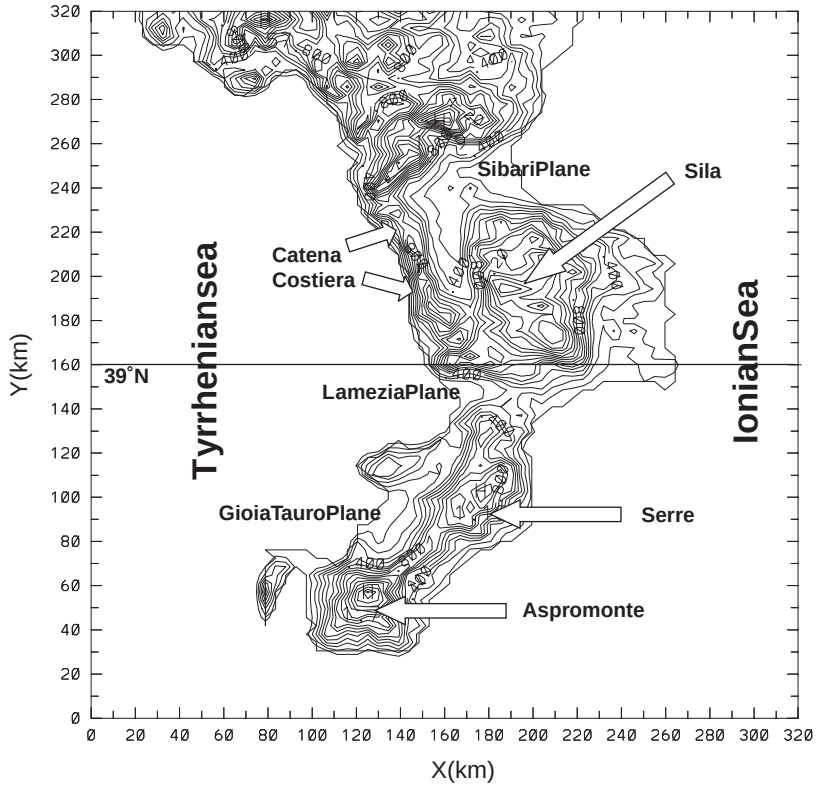

Fig. 1. – Orography of Calabria.

land breeze is a nocturnal wind, blowing from land toward sea. Both sea and land breezes are generated by the thermal difference between an air column above the sea and an air column above the land. Over a peninsula, two breeze cells develop on both sides and they can interact, provided that the peninsula width is less than two times a Rossby radius, that, at middle latitudes, is 100 km every kilometer of CBL depth.

Whenever a contrast by mountain valley is present, an upslope flow (anabatic wind) develops in clear sky days. Such winds blow from the valley to the mountain. Opposed to upslope flow nocturnal downslope wind (katabatic wind) blows from mountain to valley. Also the anabatic and katabatic winds are determined by the thermal gradient existing between an air column above mountain and an air column above valley. Whenever a peninsula covered by mountains is considered both mountain valley and sea breeze winds develop. Several studies can be found in the literature on sea breeze and local winds, some of them being reported in Simpson [1].

Calabria, that is a mountainous peninsula about 50 km wide in the WE direction located in the Central Mediterranean basin, seems to be a particularly interesting region for studying the development of such thermally induced mesoscale circulation (TFMCs). Owing to the specificity of Mediterranean climate and to the topographic characteristics of the peninsula (*i.e.* the presence of high mountains along it) intense local wind circulation can develop, above all in fair weather days which are common during summertime in the Mediterranean basin. Therefore the present study refers to such a season.

In order to better analyse breeze circulation over Calabria, we first give a brief description of the topographical features of the peninsula and then we discuss briefly the climatic contest in which the peninsula is embedded. Calabria ranges between 38°12′ and 40° latitude north, and between 16°30′ and 17°15′ longitude east (fig. 1). The west coast of Calabria is bounded by the Tyrrhenian sea, and the south and the east coasts by the Ionian sea. The Apennines run north to south all along the peninsula, characterised by four main topographical features reaching 1.5 km to 2.0 km: Catena Costiera, Sila, Le Serre, Aspromonte; with four main peaks: Montalto located in Aspromonte, Pecoraro located in Serre, Botte Donato located in Sila and Serra Dolce Dorme north of Catena Costiera (Coastal Ridge). The width of Calabria ranges from 50 to 80 km and reaches its minimum in the pass of Marcellinara, a gap between Sila and Le Serre, where the distance between the Tyrrhenian and the Ionian sea is only 30 km. Three main valleys are located close to the sea: Sibari, on the east coast along the Ionian sea, and Gioia Tauro and Lamezia on the west coast along the Tyrrhenian sea. Most of agricultural and industrial sites are located in these valleys. In the interior, the Crati river valley is located between Catena Costiera and Sila. According to such a brief description of the Calabrian topography it follows that:

1) with clear sky conditions sea breezes develop on both sides of the peninsula;

2) with clear sky conditions mountain-plane flows develop all over the peninsula;

3) sea breeze and mountain-plane circulation interact with each other and breeze circulation from the west side interacts with breeze coming from the east side.

According to a previous energetic study [2] it follows that over Calabria the intensity of the mountain-plane flows and of the sea breezes are comparable with each other. Hence, the local mesoscale flows are strongly driven by the mountains. In addition, owing to mountain symmetry with respect to the Ionian and Tyrrhenian sea, the sea breeze and mountain-plane circulations act in phase with each other and it should be expected a resulting breeze stronger than in the case of non-interacting sea breeze and mountain valley flow.

Mediterranean climate is the second factor that favours the development of local circulation. The climate of the Mediterranean basin is mainly determined by three features: topography, the baric configuration, and warm sea. While the effect of the first feature is the channelling of air masses that enter the Mediterranean basin, the other two features are very important for determining the development of the breeze circulation over Calabria.

During summer, the presence of Azores anticyclone, which covers the western and central parts of the Mediterranean basin, determines fair weather days, large-scale calm conditions and absence of rainfall [3,4]. Such weather conditions are quite often recorded in Mediterranean basin countries such as Calabria. Table I shows the observed number of sunshine hours, and their fraction of the astronomical insolation with clear sky condition, as observed at three different ground stations and in different seasons. The stations are Cecita, Crotone, and Catanzaro, respectively. As shown from table I, the fraction of the observed sunshine hours compared to the astronomical insulation are larger in summer than in winter due to smaller cloud coverage. Hence summer favours breeze circulation in the Mediterranean basin. Some other important characteristics of Mediterranean meteorology are related to the exchange of both heat and water vapour between air and sea. In fact, the sea transfers heat and water vapour to the overlying atmosphere. In

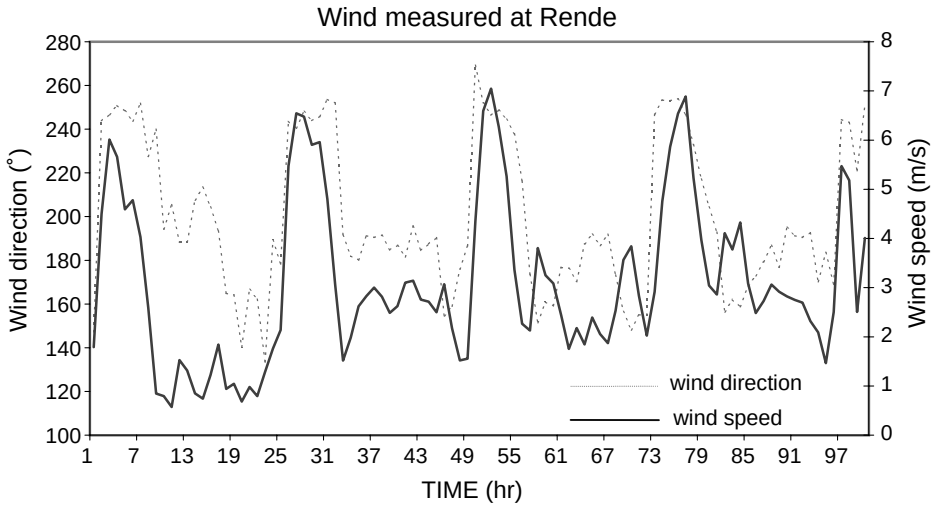

Fig. 2. – Wind speed and direction, measured at the University of Calabria (Rende) from 19 July 1997, 1100 LST, through 23 July 1997, 1500 LST. During this period of time strong TFMCs developed over the Crati Valley.

table II the monthly evaporation values (in mm/day) of the Mediterranean sea are shown. The Mediterranean basin is divided in three parts: WE (western Mediterranean), CE (central Mediterranean), EM (eastern Mediterranean). Evaporation is larger in summer than in winter, due to sea surface temperature. Such an effect determines a greater atmospheric water vapour content in summer than in winter as shown in Kalnay [5]. The enhanced water vapour content of the summer atmosphere has an important impact over Calabria, as the breeze circulation advects a large amount of water vapour over the main peaks. Moreover, when the breezes are fully developed, cumulus clouds can eventually develop. All factors aforementioned, referring to both the climatic contest of the Mediterranean basin in summer and the peculiar topography of Calabria, suggest that the summer mesoscale climate in Calabria is controlled by sea breeze and by mountain-valley flows. Such local eolic regimes are observed under calm or quasi calm large-scale conditions and with clear sky, that are frequent in Calabria. Figure 2 shows the wind speed and its direction measured at meteorological ground station of University of

TABLE I. – *Observed sunshine, hours and their fraction computed with respect to astronomical insulation in clear sky, in three different ground stations in Calabria. These data also show the effect of cloud coverage in different seasons.*

Season	**Cecita**	**Cecita** %	**Crotone**	**Crotone** %	**Catanzaro**	**Catanzaro** %
Season	F	F %	F	F %	F	F %
Winter	333	40	393	48	400	48
Spring	566	49	617	54	553	48
Summer	856	69	876	71	935	75
Autumn	485	50	554	59	491	51

TABLE II. – *Monthly evaporation values averaged over the Mediterranean sea in millimetres per day (mm/day): the basin was divided in three parts: WM (Western Mediterranean), CM (Central Mediterranean), EM (Eastern Mediterranean), adapted from Colacino 1992.*

	Jan	**Feb**	**Mar**	**Apr**	**May**	**Jun**	**Jul**	**Aug**	**Sep**	**Oct**	**Nov**	**Dec**
WM	3.0	2.7	2.0	1.9	1.8	2.2	2.8	3.5	2.6	2.8	3.2	3.5
CM	3.2	3.1	2.4	2.1	2.1	3.1	4.4	5.6	4.3	3.9	3.5	4.0
EM	4.6	4.1	3.3	2.4	2.7	3.6	5.7	6.4	6.4	4.9	4.5	4.6
Mean	3.6	3.3	2.6	2.1	2.2	3.0	4.3	5.2	4.4	3.9	3.7	4.0

Calabria beginning on 19 July 1997 at 1100 LST and ending on 23 July 1997 at 1500 LST. The station is located within the Crati valley (Rende town). During all these days strong TFMCs developed over the Crati valley and their intensity was considerable. Such a kind of circulation is typical over this valley: statistics made by measurements collected by meteorological ground station of University of Calabria reveal that 70% of summer days are characterised by breeze circulation.

We analyse the effects produced by both the complex topography of the region and the land-sea contrast. The atmospheric flow fields have been simulated by a three-dimensional non-linear numerical mesoscale model, that uses a terrain- following vertical co-ordinate [6], in order to take into account the local complexity of the terrain. As will be later shown, the effects of the breeze circulations are significant, because the TFMCs produce the reorganisation of water vapour over Calabria, triggering the onset of cumulus cloud formation and summer rainfall over main peaks.

2. – The numerical model

A numerical model in terrain following co-ordinates and hydrostatic approximation is used. The investigation is aimed to studying TFMCs. We show that the hydrostatic approximation is almost adequate for TFMCs that form and develop over Calabria. The linearized primitive equations [7], reduced to an equation for the streamfunction ψ, is

$$\left[\left(\frac{\partial}{\partial x}+k_p\right)^2+k_0^2\right]\frac{\partial^2\psi}{\partial z^2}+\left[\left(\frac{\partial}{\partial x}+k_p\right)^2+l^2\right]\frac{\partial^2\psi}{\partial x^2}=-\frac{1}{U^2}\frac{\partial Q}{\partial x}, \tag{1}$$

$$\frac{\partial\psi}{\partial z}=u; \qquad \frac{\partial\psi}{\partial x}=-w, \tag{2}$$

$$Q=Q_0\sin(kx)\sin(\omega t); \qquad \psi(x,z=0)=-Uh_0\sin(kx); \qquad \omega=\frac{2\pi}{\text{day}}. \tag{3}$$

For the sake of simplicity, we assume that the diabatic forcing Q and the orography h at the lower boundary are periodic. The Fourier transform of eq. (1) is

$$\left[\left(ik+k_p\right)^2+k_0^2\right]\frac{\partial^2\varphi}{\partial z^2}-k^2\left[\left(ik+k_p\right)^2+l_0^2\right]\varphi=-\frac{ikQ}{U^2}.$$

In hydrostatic approximation the previous equation becomes

$$\left[\left(ik + k_p\right)^2 + k_0^2\right]\frac{\partial^2\varphi}{\partial z^2} - k^2 l_0^2\varphi = -\frac{ikQ}{U^2},$$

where

$$\frac{\partial}{\partial t} \equiv i\omega; \qquad \frac{\partial}{\partial x} \equiv ik; \qquad l_0^2 = \frac{N_0^2}{U^2}; \qquad k_p = \frac{i\omega}{U}; \qquad k_0 = \frac{f}{U},$$

U is the large-scale flow, l_0 is the Scorer parameter, and k_0 is the inertial wave number.

In the absence of diabatic forcing, *i.e.* with $Q = 0$, when $k_0 < k < l_0$ the perturbation is in form of stationary waves

$$\psi(x,z) = -h_0 U \sin(kx + vz); \quad v = k\sqrt{\frac{k^2 - l_0^2}{k^2 - k_0^2}} \approx k\frac{l_0}{\sqrt{k_0^2 - k^2}}, \tag{4}$$

and, when $k < k_0$ or $k > l_0$, the perturbation is in the form of stationary trapped waves:

$$\psi(x,z) = -h_0 U \sin(kx) e^{-vz}, \quad v = k\sqrt{\frac{l_0^2 - k^2}{k^2 - k_0^2}} \approx k\frac{l_0}{\sqrt{k^2 - k_0^2}}. \tag{5}$$

For such waves the hydrostatic approximation holds when $k \ll l_0$, *i.e.* when $U \ll N_0/k$. Owing to the width of the Apennines in Calabria, the hydrostatic approximation holds when $U < 10\,\mathrm{ms}^{-1}$. Lee waves, generated by narrower ridges, can become non-hydrostatic for weaker wind intensities. Our study refers to TFMCs that develop with weak large-scale flow condition.

For the sake of simplicity, in the case $Q \neq 0$, we can assume $U = 0$. The Fourier transform of (1) is

$$\left(\frac{\partial^2}{\partial z^2} - \mu^2\right)\varphi = ikQ,$$

where

$$\mu^2 = k^2\frac{N_0^2 - \omega^2}{f^2 - \omega^2} \approx k^2\frac{N_0^2}{f^2 - \omega^2}.$$

In our case $\mu^2 > 0$, therefore the perturbation is trapped and confined near the source of the perturbation; the streamfunction is

$$\varphi(k,z) = \varphi_0\left[\int_h^{z_i} \exp -\left[\mu|z - z'|\right] \mathrm{d}z' - \int_h^{z_i} \exp\left[-(\mu|z - z'|)\right] \mathrm{d}z'\right],$$

where φ_0 is the amplitude of the streamfunction, proportional to the intensity of the diabatic forcing, z_i is the depth of the CBL, and h is the orographic profile.

The CBL height is defined as the part of the troposphere that is directly influenced by surface forcings with a timescale of one hour or less. In particular, given the functional form of eq. (3) for the diabatic heating, the time evolution of CBL is

$$z_i(T) = \frac{2}{N_0^2} \int_0^T Q_0 \sin(\omega t)\, \mathrm{d}t,$$

where $t = 0$ refers to sunrise, and N_0 is the Brunt-Väisälä frequency. Since the TFMCs evolve with a time scale of a day, $\omega \ll N_0$, and the TFMCs over Calabria are essentially hydrostatic. This is not generally true for the individual convective cell. A more general proof (in the presence of large-scale flow, orography, diabatic heat and dissipation) can be derived by the theory presented in Dalu *et al.* [7].

The model utilised for simulating the dynamic and thermodynamic fields over Calabria is a hydrostatic, incompressible form of the Colorado State University Mesoscale Model (CSUMM) described in Pielke [8], Mahrer and Pielke [9, 10], McNider and Pielke [11] and Pielke [12]. The main equations integrated by the model are momentum's, energy's, mass, and specific humidity's. Such equations are written for a terrain following co-ordinate system z^*, in order to account for the complex orography of the region. The vertical co-ordinate z^* [6] is defined as

$$z^* = \frac{\bar{s}(z - z_\mathrm{G})}{(s - z_\mathrm{G})}, \tag{6}$$

where $\bar{s}$ is the initial height of the top material surface and s is its height at a given time.

The equations in the (x, y, z^*) co-ordinate system are:

1) that one along x-momentum equation:

$$\frac{\mathrm{d}u}{\mathrm{d}t} = fv - fv_\mathrm{g} - \theta\frac{\partial \pi}{\partial x} + g\frac{z^* - \bar{s}}{\bar{s}}\frac{\partial z_\mathrm{G}}{\partial x} - g\frac{z^*}{\bar{s}}\frac{\partial s}{\partial x} + \left(\frac{\bar{s}}{s - z_\mathrm{G}}\right)^2 \frac{\partial}{\partial z^*}\left(K_z^m \frac{\partial u}{\partial z^*}\right) + \\ + \frac{\partial}{\partial x}\left(K_H \frac{\partial u}{\partial x}\right) + \frac{\partial}{\partial y}\left(K_H \frac{\partial u}{\partial y}\right); \tag{7}$$

2) that one along y-momentum equation:

$$\frac{\mathrm{d}v}{\mathrm{d}t} = fu - fu_\mathrm{g} - \theta\frac{\partial \pi}{\partial y} + g\frac{z^* - \bar{s}}{\bar{s}}\frac{\partial z_\mathrm{G}}{\partial y} - g\frac{z^*}{\bar{s}}\frac{\partial s}{\partial y} + \left(\frac{\bar{s}}{s - z_\mathrm{G}}\right)^2 \frac{\partial}{\partial z^*}\left(K_z^m \frac{\partial v}{\partial z^*}\right) + \\ + \frac{\partial}{\partial x}\left(K_H \frac{\partial v}{\partial x}\right) + \frac{\partial}{\partial y}\left(K_H \frac{\partial v}{\partial y}\right); \tag{8}$$

3) the hydrostatic equation:

$$\frac{\partial \pi}{\partial z^*} = -\frac{s - z_\mathrm{G}}{\bar{s}}\frac{g}{\theta}, \tag{9}$$

4) the energy equation:

$$\frac{\mathrm{d}\theta}{\mathrm{d}t} = \left(\frac{\bar{s}}{s - z_\mathrm{G}}\right)^2 \frac{\partial}{\partial z^*}\left(K_z^\theta \frac{\partial \theta}{\partial z^*}\right) + \frac{\partial}{\partial x}\left(K_H \frac{\partial \theta}{\partial x}\right) + \frac{\partial}{\partial y}\left(K_H \frac{\partial \theta}{\partial y}\right) + S_\theta, \tag{10}$$

where S_θ is the divergence of the infrared planetary radiation parameterised as in Sasamori [13];

5) the continuity equation:

$$\frac{\partial u}{\partial x}+\frac{\partial v}{\partial y}+\frac{\partial w^*}{\partial z^*}-\frac{1}{s-z_{\mathrm{G}}}\left(u\frac{\partial z_{\mathrm{G}}}{\partial x}+v\frac{\partial z_{\mathrm{G}}}{\partial y}\right)+\frac{1}{s-z_{\mathrm{G}}}\left(\frac{\partial s}{\partial t}+u\frac{\partial s}{\partial x}+v\frac{\partial s}{\partial y}\right)=0; \tag{11}$$

6) the water vapour continuity equation:

$$\frac{\mathrm{d}q}{\mathrm{d}t}=\left(\frac{\bar{s}}{s-z_{\mathrm{G}}}\right)^2\frac{\partial}{\partial z^*}\left(K_z^q\frac{\partial q}{\partial z^*}\right)+\frac{\partial}{\partial x}\left(K_H\frac{\partial q}{\partial x}\right)+\frac{\partial}{\partial y}\left(K_H\frac{\partial q}{\partial y}\right), \tag{12}$$

where θ is the potential temperature and π is the Exner function:

$$\pi=c_p\left(\frac{p}{p_0}\right)^{R/c_p}, \tag{13}$$

where R is the air gas constant, c_p is the specific heat of dry air at constant pressure and $p_0=1000\,\mathrm{mbar}$. In eq. (12) no source and sink terms are considered for the water vapour budget. This approach was designed for the sake of simplicity, and because our considerations refer to the redistribution of water vapour, in summer, by breeze circulation over Calabria.

An additional equation for the free surface is derived by integrating vertically the continuity equation from $z^*=0$ to $z^*=\bar{s}$ with the boundary condition $w^*=0$ on both surfaces:

$$\frac{\partial s}{\partial t}=-\frac{1}{\bar{s}}\int_0^{\bar{s}}\left[\frac{\partial}{\partial x}(u(s-z_{\mathrm{G}}))+\frac{\partial}{\partial y}(v(s-z_{\mathrm{G}}))\right]\mathrm{d}z^*. \tag{14}$$

The surface temperature is calculated solving the surface energy budget equation by the Raphson-Newton method. The surface energy balance equation is

$$v\left(\frac{\partial T}{\partial z}\right)_{\mathrm{G}}-\rho c_p u_*\theta_*-\rho L_v w_* q_*-\sigma T_{\mathrm{G}}^4+R_{\mathrm{s}}+R_{\mathrm{L}}=0. \tag{15}$$

The short-wave and long-wave radiation terms are as in Mahrer and Pielke [9]. Equation (15) is solved interactively with the equations for the long- and short-wave radiation balance, and the latent and sensible heat equation in the atmosphere.

As far as the surface energy balance equation is considered, the latent heat flux is computed by assuming uniform soil humidity distribution through six layers, equally spaced at $\Delta z=5\,\mathrm{cm}$. At initial time, the temperature and humidity in the soil are assumed constant through such six layers. Then, the temperature is updated according the diffusion equation:

$$\frac{\partial T}{\partial t}=v_{\mathrm{g}}\frac{\partial^2 T}{\partial z^2}, \tag{16}$$

where v_{g} is soil thermal diffusivity. Soil humidity is constant through the entire simulation, and its value (which is 15% of the saturation value) is used only for computing v_{g}. With the deep soil T is constant.

The lateral conditions at the inflow boundary are

$$\left.\frac{\partial(\theta,\pi,z_{\mathrm{G}},s,q)}{\partial x}\right|_n = \left.\frac{\partial(\theta,\pi,z_{\mathrm{G}},s,q)}{\partial y}\right|_n = 0, \qquad u=\bar{u}, \qquad v=\bar{v}. \tag{17}$$

Hereafter the symbol $|_n$ indicates that only the gradient component normal to every boundary must vanish. In the previous equations $\bar{u}$, $\bar{v}$, are initialised by imposing that the stress, Coriolis and pressure gradient forces are in balance with each other:

$$\frac{\partial}{\partial z}\left(K_z^m\frac{\partial\bar{u}}{\partial z}\right)+f(\bar{v}-v_{\mathrm{g}})=0, \tag{18}$$

$$\frac{\partial}{\partial z}\left(K_z^m\frac{\partial\bar{v}}{\partial z}\right)-f(\bar{u}-u_{\mathrm{g}})=0. \tag{19}$$

The lateral conditions at outflow boundaries are

$$\left.\frac{\partial(\theta,\pi,z_{\mathrm{G}},s,q)}{\partial x}\right|_n = \left.\frac{\partial(\theta,\pi,z_{\mathrm{G}},s,q)}{\partial y}\right|_n = 0, \tag{20}$$

$$\left.\frac{\partial(u,v)}{\partial x}\right|_n = \left.\frac{\partial(u,v)}{\partial y}\right|_n = 0. \tag{21}$$

The domain extends for 320 km in N-S and 320 km in E-W (fig. 1) direction. The horizontal resolution is $\Delta x=\Delta y=3.33$ km with 16 vertical levels unequally spaced starting at the surface up to 13000 m. A rigid lid is assumed at model top with a Rayleigh absorbing layer above 7000 m. Such a boundary condition absorbs spurious gravity waves and it considerably reduces reflection from the upper part of simulated domain. The time step is 15 s and the total integration time is 24 h starting at 0800 LST.

3. – Results

As said in the introduction the simulations are relative to summertime, when the local circulation prevails. Our simulations are performed in climatological conditions that are representative of July meteorological conditions [5]. Nevertheless, due to the solar zenith angle time variability, to run the model we need to select a particular day that, in the reported simulations, is the 7 July. The synoptic scale wind is assumed negligible near the ground, although different from zero ($u_{\mathrm{g}}=0.0\,\mathrm{ms}^{-1}$; $v_{\mathrm{g}}=0.5\,\mathrm{ms}^{-1}$) for jumpstarting the surface fluxes that allow to initialise the friction velocity u^*, θ^*, q^*. In the present section we analyse two simulations. In the first one the synoptic scale wind shear is zero and the large-scale flow is negligible over the entire domain. In the second the wind is assumed with a vertical shear of $1.2\,\mathrm{mkm}^{-1}\mathrm{s}^{-1}$. Such a value has been taken from the analysis of wind maps over Central Mediterranean reported in the NCEP/NCAR 40 years reanalysis project [5]. The atmospheric static stability is about $\beta=\partial\theta/\partial z=2\,\mathrm{Kkm}^{-1}$. The large-scale condition resulting from such data allows for the fully development of TFMCs.

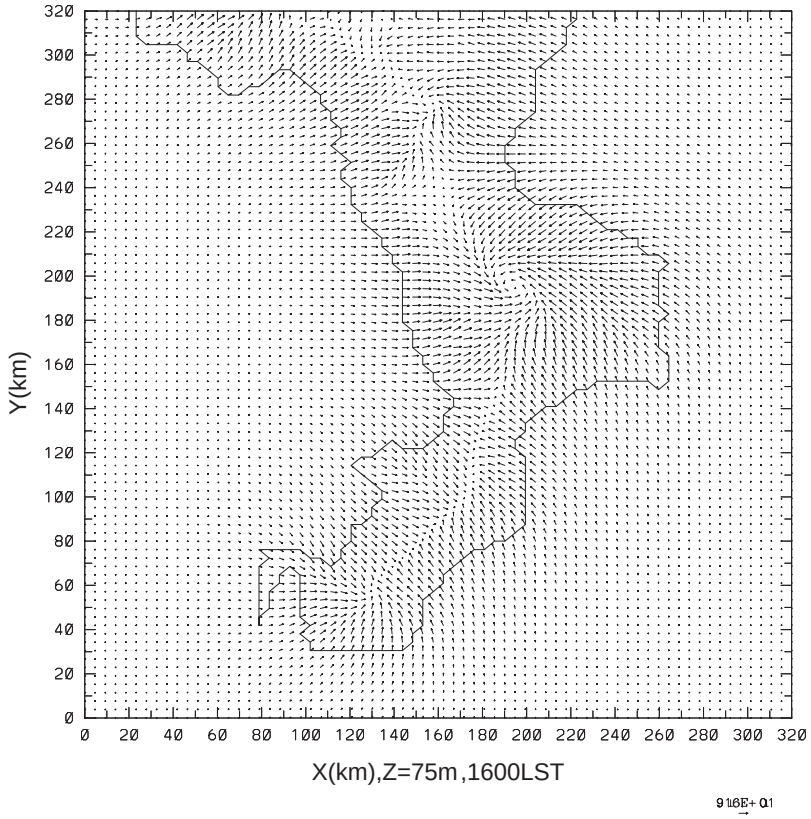

Fig. 3. – Wind vector at 75 m in the terrain-following co-ordinate system, for 16 July at 1600 LST. The four main convergence areas are associated with the four main peaks of the region. $u_g = 0.0\,\mathrm{ms}^{-1}$, $v_g = 0.5\,\mathrm{ms}^{-1}$, $\beta = 2\,\mathrm{Kkm}^{-1}$ (no wind shear).

While the first simulation is intended as a reference for future simulations over Calabria, the second is more representative of synoptic scale conditions over this region in July.

In fig. 3 we show the 16.00 LT pattern of wind vector at 75 m above ground for the first simulation (no wind shear). A strong convergence of air masses in the interior is evident. There are four main convergence peaks associated with the mountains, from north to south, Serra Dolce Dorme, Botte Donato, Monte Pecoraro, Montalto. There are also two main convergence axes associated in northern Calabria with the chain Catena Costiera and in the southern Calabria with the Calabrian Appennines range. At this time, the mesoscale flow is at its maximum and the simulated wind speeds are more than $9\,\mathrm{ms}^{-1}$. The boundary layer height (not shown), which is computed by the model following the scheme suggested by Deardroff [14, 15], is more than 2 km along large parts of the peninsula, a fact that suggests that the breeze circulation cells extension should be about 200 km. This is due to the sea breeze, that has an extension of two Rossby radii $R_0 = z_i(N_0/f)$ [16, 17]. Since N_0/f is 10^2 in mid latitudes, the Rossby radius is about 100 km for each 1000 m of the CBL z_i. Nevertheless, the simulated breeze cells extension (fig. 3) is not wider than 80 km. This is due to the peculiar shape of Calabria,

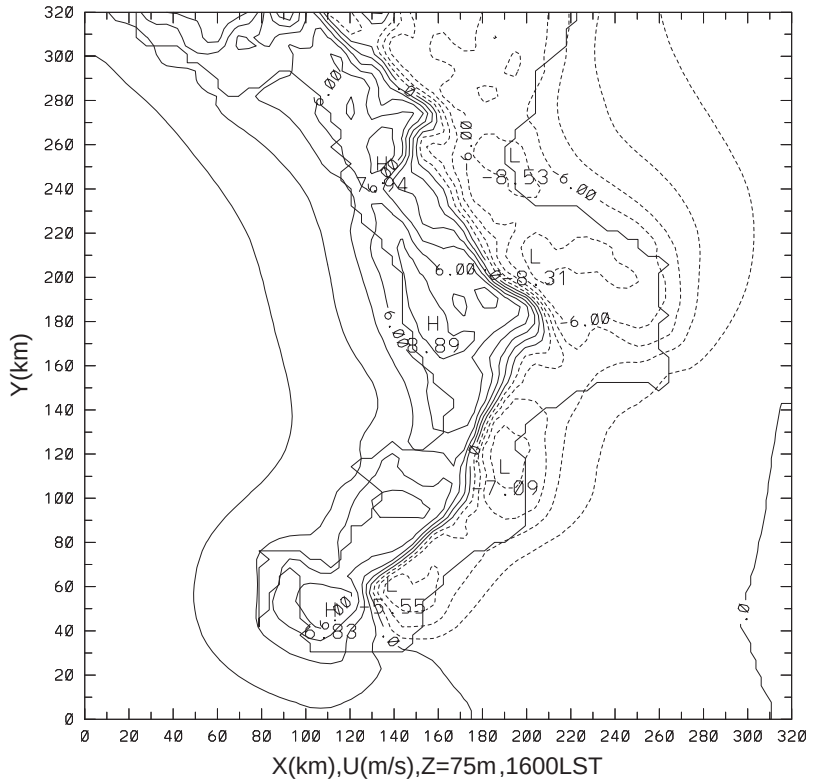

Fig. 4. – Time and day as in fig. 3 but for the zonal wind at 75 m in the terrain-following co-ordinate system. Two main axes of convergence, associated in the north part of the region with Catena Costiera and in the south part with Appennino Calabrese, respectively, are formed by TFMCs. $u_g = 0.0\,\mathrm{ms}^{-1}$, $v_g = 0.5\,\mathrm{ms}^{-1}$, $\beta = 2\,\mathrm{Kkm}^{-1}$ (no wind shear).

which is less extended than a Rossby radius in the W-E direction, while the TFMC coming from the East side collides and interferes with the TFMC on the West slope, limiting the TFMCs horizontal scale at sea. In fact, as shown in Federico *et al.* [2] in this case the Rossby radius is given by the extension of peninsula. If we compare fig. 3 with fig. 1 it results that the mountain-plane flow, combined with sea breeze is smooth compared to topography roughness. Although some structures are more evident in zonal wind (fig. 4) and in the vertical velocity (fig. 5) we can conclude that: 1) the intensity of mesoscale flow tends to average the effects of small valleys (where small means less than CBL height); 2) the use of a non-hydrostatic model is recommended when dealing with a complex orographic context whenever one aims at distinguishing and recognising the motions induced by every single valley.

Nevertheless the model is capable of catching evolution and structure of the main circulation cells, that develop over the peninsula, and that reorganise the water vapour over Calabria.

Figure 4 shows the zonal component u simulated at 75 m in the terrain-following co-ordinate system in the case of no wind shear. The zonal component reaches values up to $9\,\mathrm{ms}^{-1}$ indicating a strong convergence pattern in the centre of the region. It is

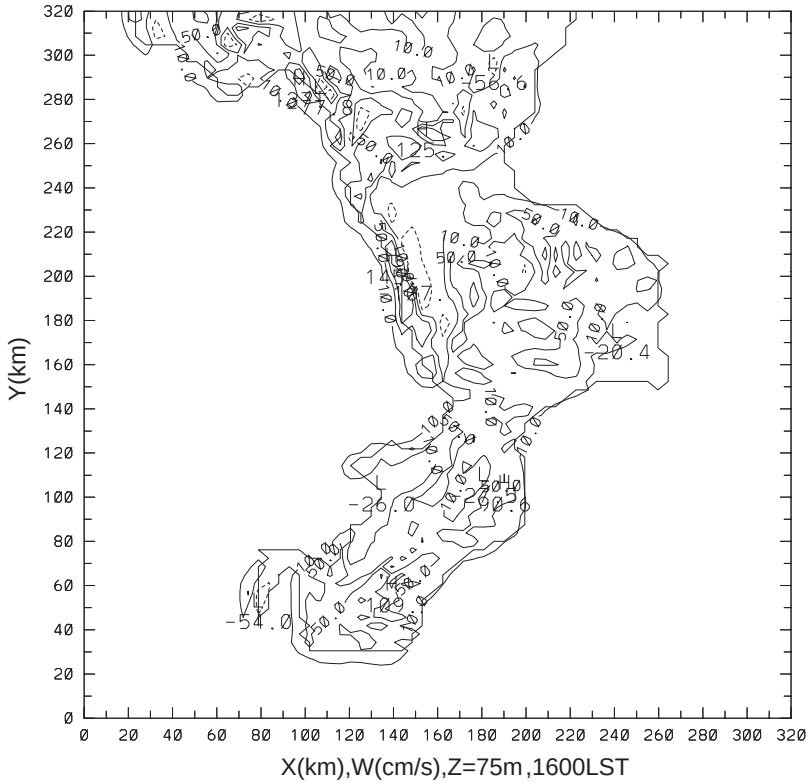

Fig. 5. – Time and day as in fig. 3 but for the vertical velocity at 75 m in the terrain-following co-ordinate system. $u_g = 0.0\,\mathrm{ms}^{-1}$, $v_g = 0.5\,\mathrm{ms}^{-1}$, $\beta = 2\,\mathrm{Kkm}^{-1}$ (no wind shear).

also evident that the flow pattern is somewhat complex, and it is closely related to the complexity of both the terrain and the mountain's profile. Since there are several mountain ranges with different horizontal scales and topographic heights, different upslope circulations with different scales can result being thermally induced.

Convergence and strong updrafts, associated with the horizontal wind pattern can be observed, that organise and lift humid marine air. Figure 5 shows the vertical velocity at 75 m above the ground for the no wind shear simulation. Vertical velocities reach, over the four main convergence peaks, intensity of (North to South) $1.25\,\mathrm{ms}^{-1}$, $0.6\,\mathrm{ms}^{-1}$, $0.9\,\mathrm{ms}^{-1}$, $1.09\,\mathrm{ms}^{-1}$, respectively and over the Catena Costiera simulated maximum of $1.45\,\mathrm{ms}^{-1}$. The vertical velocity is, except in the Crati valley, positive due to the low level horizontal convergence pattern. A downwelling in the Crati valley is due to the strong valley breeze induced by the Catena Costiera and by Sila on its East and West side, respectively.

The humid marine air is organised by TFMCs: first, the air is exported inland by sea breeze, then is lifted by the upslope mesoscale flow. Such a flow pattern has very important climatological consequences, as it favours the thermally induced development of convective systems. Thermally induced thunderstorms have a chance to occur over Calabria also in winter time, but their frequency is maximum in summer. Figures 6, 7 show the role played by local thermally induced circulations over Calabria in determining

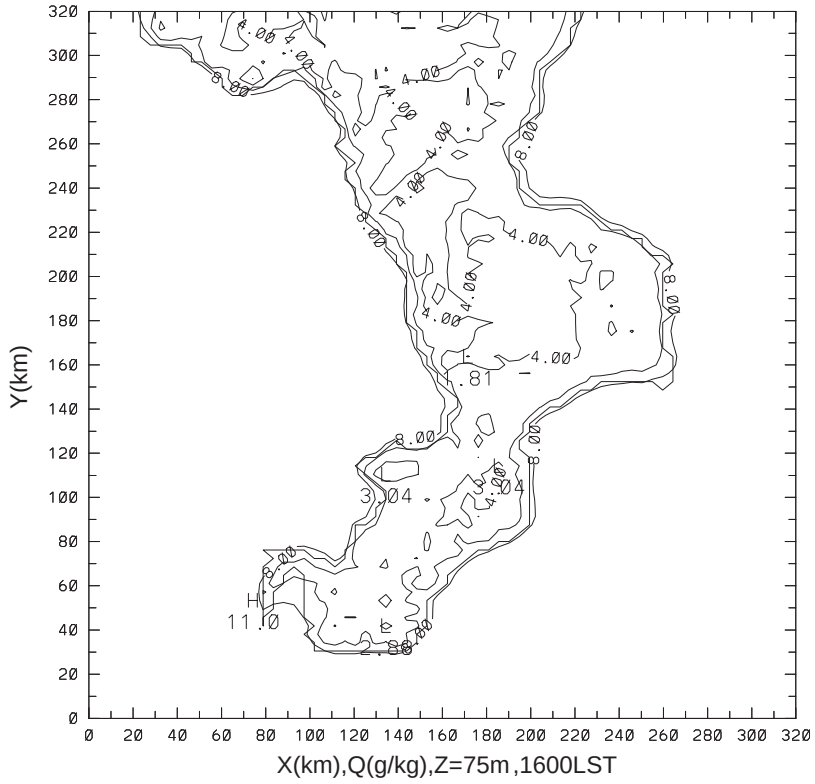

Fig. 6. – Time and day as in fig. 3 but for specific humidity at 75 m in the terrain-following co-ordinate system. $u_g = 0.0\,\mathrm{ms}^{-1}$, $v_g = 0.5\,\mathrm{ms}^{-1}$, $\beta = 2\,\mathrm{Kkm}^{-1}$ (no wind shear).

water vapour distribution. These figures show air specific humidity at 75 m and 2800 m above the ground, respectively, for the case of no wind shear. At comparatively lower levels, the mixing induced by solar heating tends to decrease the specific humidity over land and to increase water vapour content at upper levels. In fig. 7 the asymmetric distribution is also evident in the specific humidity induced by strong upslope flow associated with Catena Costiera in the N-W part of the peninsula.

Figure 8 shows the specific humidity at 2800 m above ground for the wind sheared simulation. The water vapour content reaches values greater than $7\,\mathrm{gkg}^{-1}$. Compared to fig. 7, fig. 8 shows a lesser symmetry, due to wind shear. The higher water vapour values are concentrated on the lee side of the mountains. Figure 9 shows for the wind sheared case the simulated potential temperature at the same level as in fig. 8. Asymmetries by the wind shear are evident also in this figure. Values as high as 298 K are reached over the lee side of Calabria. By adopting the values reported in figs. 7 and 8, it is possible to conclude that cumulus clouds have a chance to form over Calabria in summer, due to the redistribution of water vapour by TFMCs. In addition, asymmetries arise due to vertical wind shear. The same result can be obtained also for the no wind shear case.

The distribution of specific humidity within highest levels is also related to wind distribution. Figure 10 shows wind intensity at 2800 m in the non-zero wind shear simulation. The maximum intensity of divergent flow is, approximately, $9\,\mathrm{ms}^{-1}$.

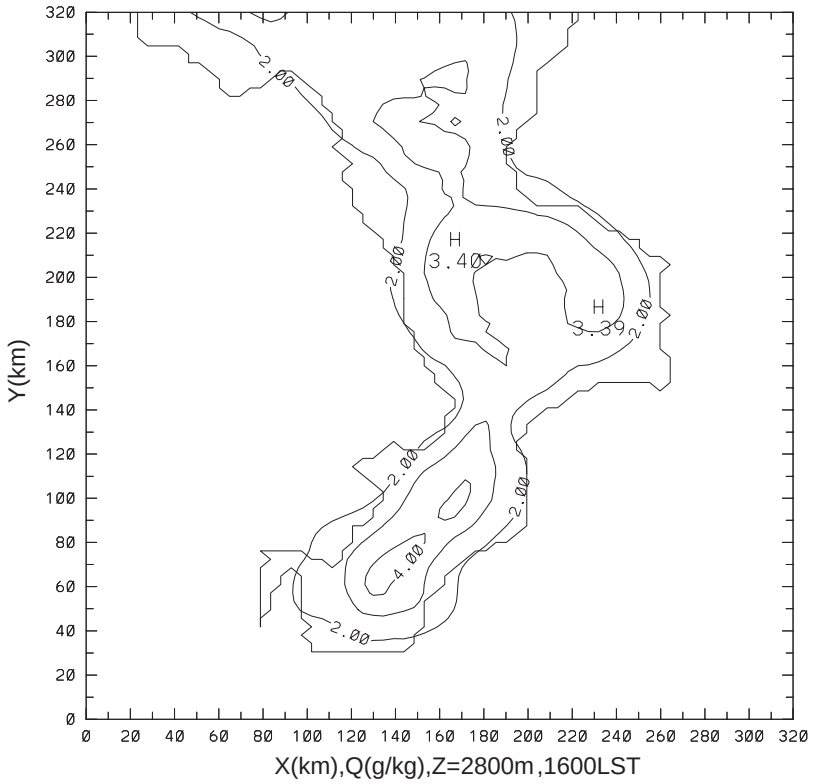

Fig. 7. – Time and day as in fig. 3 but for the specific humidity at 2800 m in the terrain-following co-ordinate system. The humid marine air is reorganized by TFMCs in order to produce local specific humidity maxima in correspondence of the higher peaks. $u_g = 0.0\,\mathrm{ms}^{-1}$, $v_g = 0.5\,\mathrm{ms}^{-1}$, $\beta = 2\,\mathrm{Kkm}^{-1}$ (no wind shear).

Wind divergence at 2800 m above ground is shown in fig. 11 for the sheared wind simulation. As far as the water vapour content is concerned the differences between simulations mainly occur in asymmetries induced by wind shear. In particular, over the Le Serre, the return flow associated with a breeze circulation is not comparatively more evident on the upstream mountain side.

The TFMCs are stronger in summer than in winter, due to the larger solar heating (that produces larger sensible fluxes) and to the weakness of large-scale flow. Figure 12 shows the sensible heat fluxes simulated at 1600 LST, negative fluxes are upwards. The simulated values are larger than $300\,\mathrm{Wm}^{-2}$ and the ratio between simulated fluxes in summer and winter ranges from 2.0 to 3.0.

Figure 13 shows the trajectories, projected into the X-Z plane, followed by two air parcels starting from the Tyrrhenian and Ionian sea, respectively, as computed from the simulated wind velocity (no shear case). At the start, several air parcels are labelled in the simulation, and their trajectories updated, every time step, by using the wind field simulated by the model. The initial positions of two such parcels in fig. 13 are, in the X-Y plane (fig. 1) (100 km, 183 km) and (230 km, 183 km) and their initial height is about 1 km above bottom boundary. The first parcel is over the Tyrrhenian sea, while

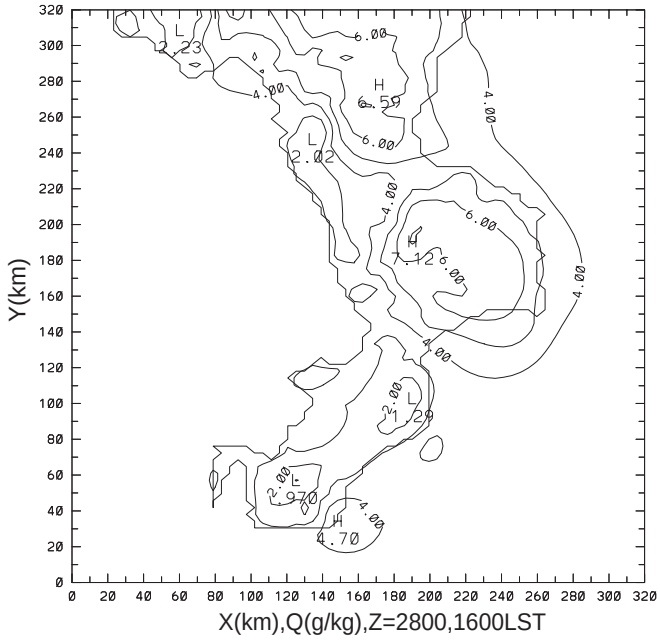

Fig. 8. – As in fig. 7 but for the sheared wind case.

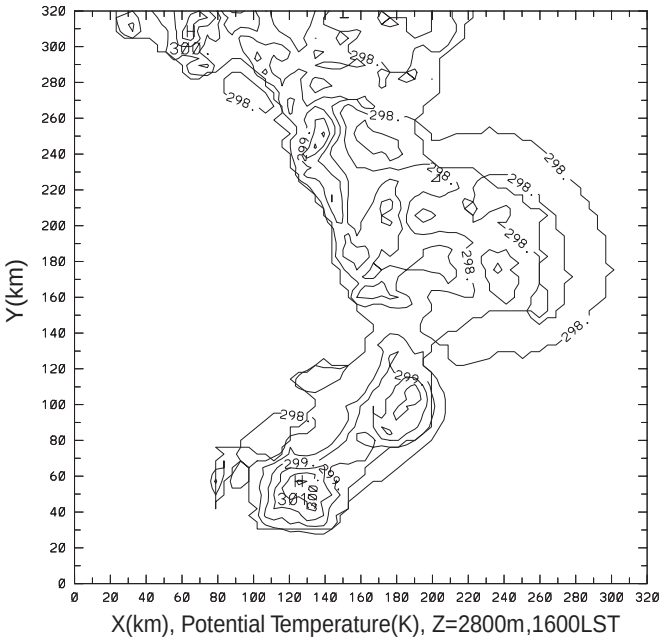

Fig. 9. – Potential temperature (K) simulated at 2800 m above ground level at 1600 LST for the wind sheared case. The analysis of fig. 8 and fig. 9 shows that cumulus clouds have a chance to form over the main peaks.

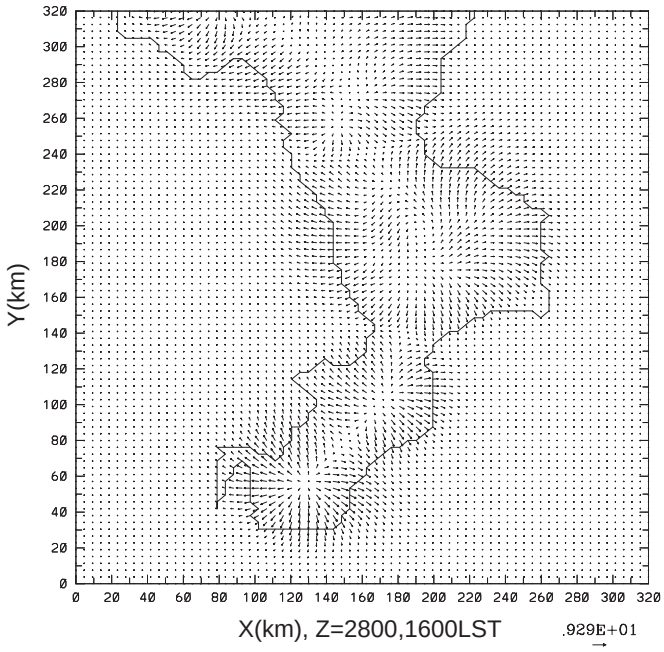

Fig. 10. – Time and day as in fig. 3 but for the wind vector at 2800 m in the terrain-following co-ordinate system. $u_g = 0.0\,\mathrm{ms}^{-1}$, $v_g = 0.5\,\mathrm{ms}^{-1}$, $\beta = 2\,\mathrm{Kkm}^{-1}$ (no wind shear).

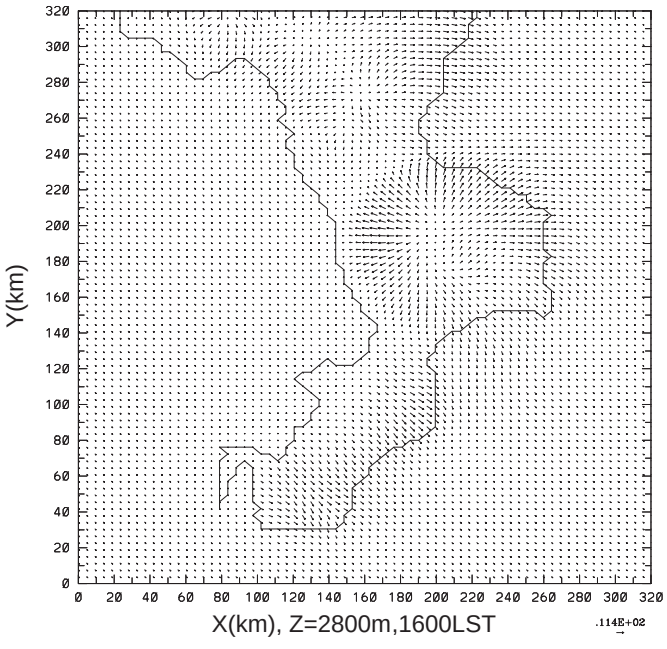

Fig. 11. – As in fig. 10 but for the sheared wind case.

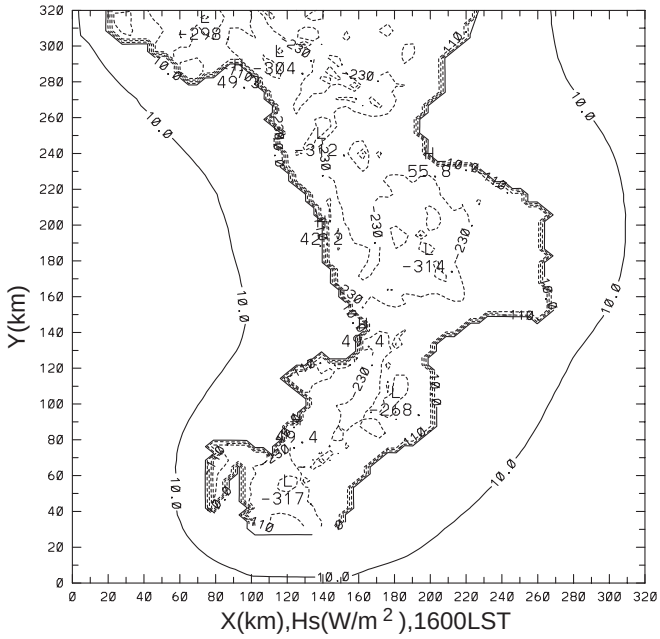

Fig. 12. – Time and day as in fig. 3 but for the sensible heat flux. Dashed contours are upwards. $u_g = 0.0\,\mathrm{ms}^{-1}$, $v_g = 0.5\,\mathrm{ms}^{-1}$, $\beta = 2\,\mathrm{Kkm}^{-1}$ (no wind shear).

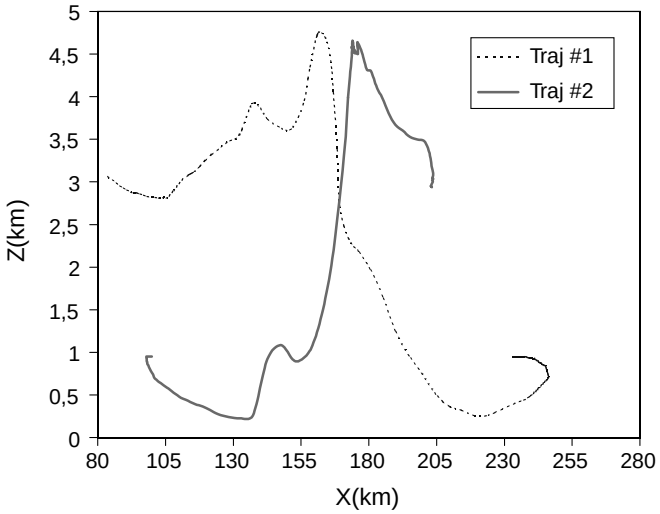

Fig. 13. – X-Z cross-section of the trajectories followed by two air parcels starting from Ionian and Tyrrhenian sea, respectively, at 600 am (no wind shear). The parcels reach the Calabria peninsula in the afternoon and are raised by TFMCs above 4 km a.s.l.

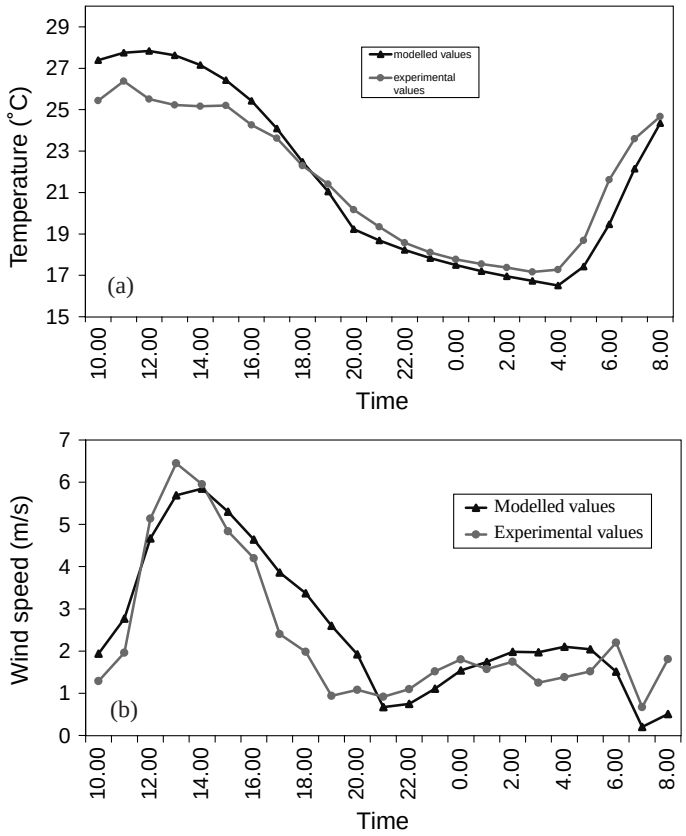

Fig. 14. – a) Observed temperature (°C) at the University of Calabria meteorological ground station, compared with the modelled field at the same location. The comparison starts at 1000 am and stops after 22 hours. The measured and simulated data are for 7 July 1997. b) Observed wind at the University of Calabria meteorological ground station, compared with the modelled field at this location. The comparison starts at 1000 am and stops after 22 hours. The measured and simulated data are for 7 July 1997.

the second is over the main land, close to the East coast of Calabria. Starting at 0600 am from the Tyrrhenian sea, the first parcel reaches the mainland in the afternoon (about 1400 LST); afterward it is raised upwards. The second parcel is first transported toward the sea by land sea flow that develops in the early morning and afterwards comes back toward the mainland (about 1230 LST). As shown in fig. 13 such air parcels usually raise up to 4 km above sea level. The parcel displacement in the meridional direction in less than 40 km and their trajectories are determined, mainly, by the local circulation induced by Sila. Air masses in fig. 13 have an initial temperature of 18 °C and a water vapour mixing ratio between 5 and 6 grkg^{-1}. Assuming, for the sake of simplicity, that every air parcel undergoes an adiabatic expansion during the raise it can be concluded that their lifting condensation level is between 2.0 and 3.0 km above sea level. Therefore convective clouds have a chance to form over Calabria.

In table III we report the total summer (June, July, August) rainfall measurements, averaged over 1951-1980 for several stations in Calabria. Monte Scuro is located in the

TABLE III. – *Total summer rainfall averaged over years 1951-1980 for several stations in Calabria, adapted after Colacino et al., 1997.*

Station	**Height Above sea level (m)**	**Total summer rain fall (mm)**
Paola	42	64
Calopezzati	180	39
Crotone	161	21
Capo Spartivento	118	22
Reggio Calabria	21	30
Monte Scuro	1720	100

centre of the region on Sila representing a mountain station where breezes convergence is very strong. Paola, Calopezzati, Crotone, Capo Spartivento and Reggio Calabria are located, in different parts of the region, close to the sea. The records show that, in the Monte Scuro station (*e.g.*, mountain station) the precipitation is 3 times the average recorded at sea-stations (3.6 times if we exclude the Paola station). Table III is indicative of the importance of breezes in determining the local climate.

The thermally forced mesoscale circulation can be monitored using different techniques. In particular, it can be observed from ground meteorological stations [1, 18, 19]. Following such an approach, we compare observed and simulated fields in a clear sky day in July. Observations begin on July 7, 1997 at 1000 am and stop after 24 h. The simulation, initialised from climatological data [5], starts at sunrise and stops after 30 h. Figures 14(a), 14(b) show the temperature and the wind of the University of Calabria, located in the Crati river valley, and the simulated fields, that are in good agreement with the observations. This is an interesting feature as the model is initialised by climatological data that characterise the large-scale conditions of the Mediterranean basin, while no particular triggering was considered for this day. It follows that the model is able to catch the breeze evolution over Calabria in the absence of large-scale synoptic disturbances at lower levels.

4. – Conclusions

The structure and formation of thermal mesoscale circulations under calm synoptic and clear sky conditions in Calabria have been investigated. Such a peninsula presents a particularly interesting case of local breeze circulations due to the presence of high mountains and to the symmetry of mountain chains with respect to the Ionian and Tyrrhenian sea, if we exclude Catena Costiera. Some results are presented that show the typical local scale circulations and the main mechanism for convective clouds generation. From the results obtained the main conclusions are:

– Thermal mesoscale circulations over Calabria appear very pronounced. This is originated by two basic features: first, Calabria is located in the central Mediterranean where the conditions, especially in summer, are favourable for the development of local circulations; second, the particular terrain of Calabria induces strong sea and valley breezes.

– The daytime upslope flow is very strong, due to the steepness of Apennines, and the thermally forced mesoscale flows are supported by sea-breeze. Therefore, the updraft is very strong, and since the W-E spatial scale of Calabria is less than one Rossby radius, the intensified head-on moving circulations meet in the early afternoon. The size of the circulation cells is reduced by such interaction.

– The water vapour is organised by the TFMCs and is transported into the interior, where, owing to the convergence, is uplifted, to generate convective clouds. The afore-mentioned processes can play a fundamental role in summer because fresh water over the Calabria can be supplied through the mechanisms here described. A similar mechanism was reported as responsible for large incidence of thunderstorms over several countries all over the world, and extensive studies were carried out over Florida [8, 20].

* * *

This work was partially supported by the INEA project POM - Misura 2 contract A05. We are indebted with the referees for their useful suggestions.

REFERENCES

[1] Simpson J. E., *Sea Breeze and Local Wind* (Cambridge University Press, Great Britain) 1994, p. 234.
[2] Federico S., Dalu G. A., Bellecci C. and Colacino M., *Mesoscale energetics and flows induced by sea-land and mountain-valley contrasts*, *Ann. Geophys.*, **18** (2000) 235-246.
[3] Colacino M., *Mediterranean Meteorology* in *Winds and Currents of the Mediterran*, edited by H. Charnock, *Rep. Meteorol. Oceanogr.*, **f 40** (1992) 1-38.
[4] Colacino M., Conte M. and Piervitali E., *Elementi di Climatologia della Calabria*, CNR-IFA, Roma, 1997.
[5] Kalnay E., Kanamitsu M., Klister R., Collins W., Daeven D., Gandin C., Iredell M., Saha S., White G., Wallen J., Zhu Y., Ceetnaa A., Reynolds R., Chelliah M., Ebisuzaki W., Higgins W., Janowak J., Mo K. C., Ropelewski C., Wang J., Jenne R. and Joseph D., *The NCEP/NCAR 40-year reanalysis project*, *Bull. Am. Meteorol. Soc.*, March issue, 1966.
[6] Pielke R. A. and Martin C. L., *The derivation of a terrain-following coordinate system for use in a hydrostatic model*, *J. Atmos. Sci.*, **38** (1981) 1708-1713.
[7] Dalu G. A., Pielke R. A., Baldi M. and Zeng X., *Heat and momentum fluxes induced by thermal inhomogeneities with and without large-scale flow*, *J. Atmos. Sci.*, **53** (1996) 3286-3302.
[8] Pielke R. A., *A three-dimensional numerical model of the sea breezes over South Florida*, *Mon. Weather Rev.*, **102** (1974) 115-139.
[9] Mahrer Y. and Pielke R. A., *A numerical study of the air flow over irregular terrain*, *Contr. Atmos. Phys.*, **50** (1977) 98-113.
[10] Mahrer Y. and Pielke R. A., *The effects of topography on sea and land breezes in a two-dimensional numerical model*, *J. Appl. Meteor.*, **35** (1995) 1166-1169.
[11] McNider T. R. and Pielke R. A., *Diurnal boundary-layer development over sloping terrain*, *J. Atmos. Sci.*, **38** (1981) 2198-2212.
[12] Pielke R. A., *Mesoscale Meteorogical Modeling* (Academic Press, New York) 1984, p. 612.
[13] Sasamori T., *A linear harmonic analysis of atmospheric motion with radiative dissipation*, *J. Meteorol. Soc. Jpn.*, **50** (1972) 505-518.

[14] Deardroff J., *Three dimensional numerical study of the height and mean structure of a heated boundary layer*, *Bound.-Layer Meteor.*, **7** (1974) 81-106.
[15] Bellecci C., Dalu G. A., Aversa P., Casella L., Federico S. and Gaudio P., *Evolution of Water Vapour profiles Over Complex Terrain: Observation and Comparison with Model Simulations in the Valley of Cosenza*, in *SPIE Proceedings on Laser Radar Ranging and Atmospheric Lidar Techniques II*, Vol. **3865** (1999) pp. 108-118.
[16] Dalu G. A. and Pielke R. A., *An analytical study of the sea breeze*, *J. Atmos. Sci.*, **46** (1989) 1815-1825.
[17] Dalu G. A., Pielke R. A., Avissar R., Kallos G., Baldi M. and Guerrini A., *Linear impact of thermal inhomogeneities on mesoscale atmospheric flow with zero synoptic wind*, *Ann. Geophys.*, **9** (1991) 641-647.
[18] Simpson J. E., *Diurnal changes in sea-breeze direction*, *J. Appl. Meteorol.*, **35** (1996) 1166-1169.
[19] Colacino M., Dell'Osso L., *The local atmospheric circulation in the Rome area: surface observations*, *Bound.-Layer Meteor.*, **14** (1978) 133-151.
[20] Nicholls M. E., Pielke R. A. and Cotton W. R., *A two-dimensional numerical investigation of the interaction between sea breezes and deep convection over Florida peninsula*, *Mon. Weather Rev.*, **119** (1990) 298-323.